PHYSICAL REVIEW D **93,** 123520 (2016)

Geodesics of McVittie spacetime with a phantom cosmological background

Ioannis Antoniou[*] and Leandros Perivolaropoulos[†]
Department of Physics, University of Ioannina, Ioannina 45110, Greece
(Received 14 March 2016; published 21 June 2016)

We investigate the geodesics of a Schwarzschild spacetime embedded in an isotropic expanding cosmological background (McVittie metric). We focus on bound particle geodesics in a background including matter and phantom dark energy with constant dark energy equation-of-state parameter $w < -1$ involving a future big rip singularity at a time t_*. Such geodesics have been previously studied in the Newtonian approximation and found to lead to dissociation of bound systems at a time $t_{\rm rip} < t_*$, which for a fixed background w depends on a single dimensionless parameter $\bar{\omega}_0$ related to the angular momentum and depending on the mass and the size of the bound system. We extend this analysis to large massive bound systems where the Newtonian approximation is not appropriate and we compare the derived dissociation time with the corresponding time in the context of the Newtonian approximation. By identifying the time when the general-relativistic analog of the effective potential $V_{\rm eff}$ minimum disappears due to the repulsive force of dark energy, we find that the dissociation time of bound systems occurs earlier than the prediction of the Newtonian approximation. However, the effect is negligible for all existing cosmological bound systems and it would become important only in hypothetical bound extremely massive ($10^{20} M_\odot$) and large (100 Mpc) bound systems. We verify this result by explicitly solving the geodesic equations. This result is due to an interplay between the repulsive phantom dark energy effects and the existence of the well-known innermost stable orbits of Schwarzschild spacetimes.

DOI: 10.1103/PhysRevD.93.123520

I. INTRODUCTION

The simplest cosmological model that is consistent with current cosmological observations is the ΛCDM model where the observed accelerating expansion of the Universe is attributed to a cosmological constant which introduces repulsive properties to gravity at large distances [1–6]. The cosmological constant may be described as a homogeneous dark energy perfect fluid with constant energy density ρ and negative pressure p with constant equation of state

$$w = \frac{p}{\rho} = -1. \tag{1.1}$$

A generalization of ΛCDM where the cosmic acceleration is induced by a dark energy fluid with constant equation of state introduces a new parameter w in the models, which is constrained by cosmological observations at the 1σ level to be in the range [7–10]

$$-1.5 < w < -0.7. \tag{1.2}$$

Based on these constraints and in the context of the above minimal generalization of ΛCDM, there is a significant probability that $w < -1$. For such a range of w, this class of models predicts the existence of a future singularity where the scale factor diverges at a finite future time.

This behavior emerges by solving the Friedmann equation in the presence of matter density ρ_m, dark energy density ρ_x, and equation of state $p_x = w\rho_x$, which may be written as [11,12]

$$\begin{aligned}\frac{\dot{a}^2}{a^2} &= \frac{8\pi G}{3}[\rho_m + \rho_x]\\ &= H_0^2\left[\Omega_m^0\left(\frac{a_0}{a}\right)^3 + \Omega_x^0\left(\frac{a_0}{a}\right)^{3(1+w)}\right],\end{aligned} \tag{1.3}$$

and

$$\begin{aligned}\frac{\ddot{a}}{a} &= -\frac{4\pi G}{3}[\rho_m + \rho_x(1+3w)]\\ &= -\frac{4\pi G}{3}\rho_x[\Omega_x^{-1} + 3w]\\ &= -\frac{4\pi G}{3}\rho_x\left[\frac{\Omega_m^0}{\Omega_x^0}\left(\frac{a_0}{a}\right)^{-3w} + 1 + 3w\right],\end{aligned} \tag{1.4}$$

with the solution

$$a(t) = \frac{a(t_m)}{[-w + (1+w)\frac{t}{t_m}]^{-\frac{2}{3(1+w)}}}, \qquad t > t_m, \tag{1.5}$$

where t_m is the time when the dark energy density becomes larger than the matter density. Also, H_0 is the present value of the Hubble parameter and a_0 is the present value of the scale factor. For $w < -1$ the scale factor and its derivatives diverge at a finite time known as the big rip time [13–16],

[*]ianton@cc.uoi.gr
[†]leandros@uoi.gr

$$t_* = \frac{w}{1+w} t_m > 0. \tag{1.6}$$

This divergence results in a diverging repulsive gravitational force which rips apart all bound systems at times $t_{\rm rip}$ that depend on their binding energies and forms of effective potentials.

An important question to address is, what is the physical mechanism that induces this dissociation of bound systems and what is the time when the dissociation occurs as a function of w? In order to address this question, a gravitationally bound system may be represented as a single test particle bound in a circular orbit of radius r_0 by the gravitational force of a central spherical massive object of mass m. The features of the trajectory of the test particle may be obtained in any of the following ways.

(1) Using a rough comparison of the attractive gravitational force with the repulsive force induced by the expansion [13].

(2) Using a derivation of the particle trajectory using equations of motion in the Newtonian approximation which take into account the attractive gravitational force, the repulsive force due to the expansion as well as the centrifugal effects due to angular momentum [12,17–19].

(3) Using the full relativistic geodesic equations obtained from a metric that is a solution of the Einstein equations and interpolates between a Schwarzschild metric and a Friedmann-Robertson-Walker (FRW) metric. Such a metric is the McVittie metric [20]. Other approaches to such an interpolation may be found in Refs. [21–24].

Previous studies have pursued the first two approaches with results that are in qualitative agreement within a factor of 3. According to the approach of Ref. [12], the dissociation of the bound system is associated with the disappearance of the minimum of the effective potential that determines the radial motion of the test particle. This minimum disappears when the dynamics become dominated by the effects of the accelerating expansion of the phantom cosmological background. Thus the dissociation of a bound system occurs at a time $t_{\rm rip}$ given by

$$t_* - t_{\rm rip} = \frac{16\sqrt{3}}{9} \frac{T\sqrt{2|1+3w|}}{6\pi|1+w|}, \tag{1.7}$$

where T is the period of the gravitationally bound system with mass m, radius r_0, and angular velocity ω_0 of the form

$$\omega_0^2 \equiv \left(\frac{2\pi}{T}\right)^2 = \frac{Gm}{r_0^3}. \tag{1.8}$$

This result improves over the corresponding result of Ref. [13] by a factor of $16\sqrt{3}/9 \simeq 3$ because it takes into account the effects of the centrifugal term and provides a clear definition of the dissociation time as the time when the minimum of the effective potential disappears due to the domination of the repulsive gravitational effects of the expansion. On the other hand, the analysis of Ref. [12] is limited by the fact that it uses the Newtonian approximation for the dynamical equations of the particle orbits, and therefore it may not be applicable for the analysis of the dissociation of strongly bound systems like accretion disks [25,26].

In this study we extend the analysis of Ref. [12] by going beyond the Newtonian approximation and taking into account relativistic effects. In particular, we consider the full geodesics corresponding to the McVittie metric in a phantom cosmological background. Using these geodesic equations, we construct the general-relativistic analog of the effective potential corresponding to bound particle orbits and derive the time of dissociation ($t_{\rm rip}$) when the minimum of the potential disappears due to expansion effects. These results are confirmed by comparing with numerical solutions of the geodesic equations corresponding to initial circular bounded orbits. We compare these results with the corresponding results of previous studies [12] obtained in the Newtonian limit.

The structure of this paper is the following. In the next section we review the McVittie metric and its limits (FRW, Newtonian, Schwarzschild). We also analyze the form of the geodesics, define the general-relativistic analog of the effective potential that determines the dynamics of the bound orbits, and compare it with the corresponding Newtonian approximation in the context of a phantom cosmology. In Sec. III we present the numerical solution of the geodesics for various parameter values showing the dissociation of the bound systems. The times of dissociation $t_{\rm rip}$ obtained by the numerical solution are also compared with the time when the minimum of the general-relativistic analog of the effective potential disappears due to the repulsive effects of the accelerating cosmological expansion. Comparison with the corresponding Newtonian results is also made. Finally, in Sec. IV we conclude, summarize, and discuss possible extensions on this analysis.

II. GEODESIC EQUATIONS AND THEIR LIMITS

An acceptable way to describe a bound system embedded in an expanding cosmological background is provided by the McVittie metric [20]. This is a solution of the Einstein equations which represents an embedding of the Schwarzschild field in an isotropic cosmological background. For a flat cosmological background this metric is of the form

$$ds^2 = -\left(f - \frac{r^2H^2}{c^2}\right)d(ct)^2 - 2rHf^{-1/2}dtdr + f^{-1}dr^2 + r^2d\Omega^2, \tag{2.1}$$

where $m > 0$ is a constant, $d\Omega^2 = d\theta^2 + \sin^2\theta d\varphi^2$, $f = f(r) = 1 - 2Gm/(c^2 r) > 0$, and $H = H(t) = \frac{\dot{a}}{a}$ is the Hubble parameter of the cosmological background. In what follows we do not set $c = G = 1$ in order to clearly show the Newtonian limit ($c \to \infty$).

In Eq. (2.1) r is the physical spatial coordinate connected with the comoving spatial coordinate ρ as $\rho = \frac{r}{a(t)}$. Setting $m = 0$ and using the comoving coordinate, we obtain the flat background FRW metric

$$ds^2 = -(1 - r^2H^2)d(ct)^2 - 2rHdtdr + dr^2 + r^2 d\Omega^2 = -dt^2 + a^2(d\rho^2 + \rho^2 d\Omega^2). \tag{2.2}$$

Similarly, by setting $H = 0$ the metric (2.1) reduces to the Schwarzschild metric.

The Schwarzschild–de Sitter metric may also be obtained as a special case of the McVittie metric by fixing the Hubble parameter to a constant $H^2 = H_0^2 = \frac{\Lambda}{3}$ (where Λ is the cosmological constant) and performing a coordinate transformation [27]

$$X = t + u(r), \tag{2.3}$$

with

$$u'(r) = H_0 r/c\left(\sqrt{f}\left(f - \frac{r^2H^2}{c^2}\right)\right), \tag{2.4}$$

leading to the Schwarzschild–de Sitter (or Kottler) metric

$$ds^2 = -\left(1 - \frac{2Gm}{c^2 r} - \frac{\Lambda}{3}r^2\right)d(cX)^2 - \left(1 - \frac{2Gm}{c^2 r} - \frac{\Lambda}{3}r^2\right)^{-1}dr^2 + r^2 d\Omega^2. \tag{2.5}$$

In the Newtonian limit, using comoving coordinates, the McVittie metric may be written as [12,28,29]

$$ds^2 = \left(1 - \frac{2Gm}{c^2 a(t)\rho}\right)d(ct)^2 - a(t)^2(d\rho^2 + \rho^2(d\theta^2 + \sin^2\theta d\varphi^2)). \tag{2.6}$$

The Newtonian geodesics corresponding to the metric (2.6) are of the form [24,30]

$$\ddot{r} - \frac{\ddot{a}}{a}r + \frac{Gm}{r^2} - r\dot{\varphi}^2 = 0, \tag{2.7}$$

and

$$r^2\dot{\varphi} = L, \tag{2.8}$$

where r is the physical coordinate ($r = a\rho$) and L is the angular momentum per unit mass ($L = \omega r^2$, constant). Combining Eqs. (2.7) and (2.8), we find the radial dynamical equation in the Newtonian limit,

$$\ddot{r} = \frac{\ddot{a}}{a}r + \frac{L^2}{r^3} - \frac{Gm}{r^2}. \tag{2.9}$$

Notice that c does not appear in this equation since it is nonrelativistic. If we ignore the term due to the expansion, then the angular velocity of a test particle in a bound circular orbit with radius r_0 at an initial time t_0 is obtained from Eq. (2.9) as

$$\dot{\varphi}(t_0)^2 = \omega_0^2 = \frac{Gm}{r_0^3}. \tag{2.10}$$

The radius of the circular orbit will be perturbed once the expansion is turned on but the above Eq. (2.10) remains a good approximation close to the end of the era of matter domination [Eq. (2.9)] $t_m = t_0$, when the expansion repulsive force is subdominant. It is convenient to rescale Eq. (2.9) to a dimensionless form by defining the dimensionless quantities $\bar{r} \equiv \frac{r}{r_0}$, $\bar{\omega}_0 \equiv \omega_0 t_0$, and $\bar{t} \equiv \frac{t}{t_0}$. The choice of this rescaling is made so that the effect of the expansion is initially small (at time $\bar{t} = 1$) and the initial minimum of the effective potential is approximately at $\bar{r} = 1$. Typical values of $\bar{\omega}_0$ are obtained using the scale and the mass of bound systems. Thus $\bar{\omega}_0$ is $O(1)$ for a cluster of galaxies, about 200 for a galaxy, and 10^6 for the Solar System.

Assuming a constant w and using the form of the scale factor in Eq. (1.5), the radial dynamical equation (2.9) takes the form

$$\ddot{\bar{r}} + \frac{\bar{\omega}_0^2}{\bar{r}^2}\left(1 - \frac{1}{\bar{r}}\right) + \frac{2}{9}\frac{(1+3w)\bar{r}}{(-w + (1+w)\bar{t})^2} = 0. \tag{2.11}$$

From Eq. (2.11), we derive the effective radial force in the context of the Newtonian approximation,

$$F_{\text{eff}} = -\frac{\bar{\omega}_0^2}{\bar{r}^2}\left(1 - \frac{1}{\bar{r}}\right) - \frac{2}{9}\frac{(1+3w)\bar{r}}{(-w + (1+w)\bar{t})^2}, \tag{2.12}$$

and the corresponding effective potential

$$V_{\text{eff}} = -\frac{\bar{\omega}_0^2}{\bar{r}} + \frac{\bar{\omega}_0^2}{2\bar{r}^2} - \frac{1}{2}\lambda(\bar{t})^2\bar{r}^2, \tag{2.13}$$

where (for $w < -1$)

$$\lambda^2(\bar{t}) = \frac{2}{9}\frac{(1+3w)}{(-w + (1+w)\bar{t})^2}. \tag{2.14}$$

The repulsive term due to the expansion (proportional to λ^2) increases with time, and at a time $\bar{t}_{\text{rip}}$ given by Eq. (1.7) it destroys the effective potential minimum induced by the interplay between the attractive gravity and centrifugal terms. Thus a bound system gets dissociated by the expansion at $\bar{t} = \bar{t}_{\rm rip}$ [12].

This analysis made in the context of the Newtonian approximation is inappropriate for some massive large strongly bound systems where relativistic effects need to be taken into account. A proper relativistic analysis requires the use of the geodesic equations obtained from the McVittie metric (2.1). These dynamical equations are of the form [27]

$$\ddot{r} = rf^{1/2}H'\dot{t}^2 + \left(1 - \frac{3Gm}{c^2 r}\right)\frac{L^2}{r^3} - \frac{Gm}{r^2} + rH^2, \tag{2.15}$$

$$\ddot{t} = -\left(1 - \frac{3Gm}{rc^2}\right)f^{-1/2}H\dot{t}^2 - \frac{2Gm}{r^2}f^{-1}\dot{t}\,\dot{r} + f^{-1/2}H. \tag{2.16}$$

The overdot represents a derivative with respect to the proper time and the prime represents a derivative with respect to the coordinate time. A first integral of these equations may also be obtained as

$$\chi\dot{t}^2 + 2\frac{\alpha\dot{t}\,\dot{r}}{c} - \frac{f^{-1}\dot{r}^2}{c^2} - \frac{L^2}{c^2 r^2} = 1, \tag{2.17}$$

where

$$\chi(t,r) = f - \frac{r^2H^2}{c^2}, \qquad \alpha(t,r) = \frac{rf^{-1/2}H}{c}. \tag{2.18}$$

We may choose $\dot{t} > 0$ along causal geodesics and focus on the system of the radial geodesic (2.15) coupled with the first integral (2.17).

As a first step towards the investigation of this system we use a proper rescaling. In particular, we assume a background expansion model corresponding to a constant $w < -1$ [Eq. (1.5)] and rescale the system using the scales r_0 (circular orbit radius in the absence of expansion) and $t_0 = t_m$. We then define the dimensionless quantities: $\bar{t} \equiv t/t_0$, $\bar{\tau} \equiv \tau/t_0$ (τ is the proper time), $\bar{r} \equiv r/r_0$, $\bar{m} \equiv Gm/r_0c^2$, $\bar{H} \equiv Ht_0$, and $\bar{\omega}_0 \equiv \omega_0 t_0$. Using the dimensionless coordinates, the radial geodesic (2.15) and the first integral (2.17) take the form

$$\ddot{\bar{r}} = \bar{r}f^{1/2}\bar{H}'\dot{\bar{t}}^2 + \left(1 - \frac{3\bar{m}}{\bar{r}}\right)\frac{\bar{\omega}_0^2}{\bar{r}^3} - \frac{\bar{m}}{\bar{r}^2}\left(\frac{ct_0}{r_0}\right)^2 + \bar{r}\bar{H}^2, \tag{2.19}$$

$$\left[f - \left(\frac{r_0}{ct_0}\right)^2\bar{r}^2\bar{H}^2\right]\dot{\bar{t}}^2 + 2\left(\frac{r_0}{ct_0}\right)^2\bar{r}\,\bar{H}\,f^{-1/2}\dot{\bar{t}}\,\dot{\bar{r}} - \frac{\dot{\bar{r}}^2}{f}\left(\frac{r_0}{ct_0}\right)^2 - \frac{\bar{\omega}_0^2}{\bar{r}^2}\left(\frac{r_0}{ct_0}\right)^2 = 1, \tag{2.20}$$

where f is expressed in terms of $\bar{m}$ as

$$f = 1 - \frac{2\bar{m}}{\bar{r}}. \tag{2.21}$$

We now determine the scale r_0 for the relativistic case considered here and compare with the corresponding Newtonian scale. The general-relativistic analog of the effective radial force in the absence of cosmological expansion ($H = 0$) takes the form

$$F_{\rm eff} = \left(1 - \frac{3\bar{m}}{\bar{r}}\right)\frac{\bar{\omega}_0^2}{\bar{r}^3} - \frac{\bar{m}}{\bar{r}^2}\left(\frac{ct_0}{r_0}\right)^2, \tag{2.22}$$

which vanishes for ($\bar{r} = 1$)

$$\bar{\omega}_0 = \frac{ct_0}{r_0}\sqrt{\frac{\bar{m}}{1 - 3\bar{m}}}. \tag{2.23}$$

Equation (2.23) also constitutes the definition of the scale r_0 used for the rescaling of the geodesic equations. From Eqs. (2.15) and (2.23) we obtain the dimensionless form of the radial geodesic equation,

$$\ddot{\bar{r}} = \bar{r}f^{1/2}\bar{H}'\dot{\bar{t}}^2 + \left(1 - \frac{3\bar{m}}{\bar{r}}\right)\frac{\bar{\omega}_0^2}{\bar{r}^3} - \frac{(1-3\bar{m})\bar{\omega}_0^2}{\bar{r}^2} + \bar{r}\bar{H}^2. \tag{2.24}$$

Similarly, the dimensionless form of the first integral (2.17) is

$$\left[f - \frac{\bar{r}^2\bar{m}\bar{H}^2}{\bar{\omega}_0^2(1-3\bar{m})}\right]\dot{\bar{t}}^2 + \frac{2\bar{m}}{\bar{\omega}_0^2(1-3\bar{m})}\bar{r}\,\bar{H}\,f^{-1/2}\dot{\bar{t}}\,\dot{\bar{r}} - \frac{\dot{\bar{r}}^2}{f\bar{\omega}_0^2}\frac{\bar{m}}{1-3\bar{m}} - \frac{\bar{m}}{\bar{r}^2(1-3\bar{m})} = 1. \tag{2.25}$$

The Newtonian limit is obtained for $c \to \infty$, which corresponds to

$$\bar{m} \equiv \frac{Gm}{c^2 r_0} \to 0, \qquad f \to 1. \tag{2.26}$$

As expected, in this limit we obtain $\dot{\bar{t}} = 1$ from the integral equation (2.25), while the radial equation reduces to the corresponding Newtonian equation (2.9). Similarly, in this limit the scale r_0 [defined through Eq. (2.23)] reduces to the corresponding Newtonian scale [Eq. (2.10)] since $c^2\bar{m} = \frac{Gm}{r_0}$.

Therefore, assuming a fixed expanding cosmological background, the geodesics in the McVittie metric are fully determined by two dimensionless parameters $\bar{m}$ and $\bar{\omega}_0$, while the corresponding Newtonian orbits are determined by a single parameter ($\bar{\omega}_0$) and are obtained as the limit $\bar{m} \to 0$ of the relativistic orbits. The dimensionless parameters $\bar{m}$ and $\bar{\omega}_0$ are obtained from the mass m (measured in solar masses $M_\odot$) and the scale r_0 (measured in Mpc) of the physical system by the relations

$$\bar{m} \simeq \frac{5\times 10^{-20} m}{r_0}, \tag{2.27}$$

$$\bar{\omega}_0 \simeq \frac{1780}{r_0}\sqrt{\frac{\bar{m}}{1-3\bar{m}}}, \tag{2.28}$$

while the reverse relations are

$$m \simeq \frac{3.5\times 10^{22}\bar{m}}{\bar{\omega}_0}\sqrt{\frac{\bar{m}}{1-3\bar{m}}}, \tag{2.29}$$

$$r_0 \simeq \frac{1780}{\bar{\omega}_0}\sqrt{\frac{\bar{m}}{1-3\bar{m}}}. \tag{2.30}$$

In the Schwarzschild limit ($H=0$) the radial geodesic equation becomes

$$\ddot{\bar{r}} = \left(1-\frac{3\bar{m}}{\bar{r}}\right)\frac{\bar{\omega}_0^2}{\bar{r}^3} - \frac{(1-3\bar{m})\bar{\omega}_0^2}{\bar{r}^2}. \tag{2.31}$$

The general-relativistic analog of the effective radial force has two roots given by

$$\bar{r} = 1, \qquad \bar{r} = \frac{3\bar{m}}{1-3\bar{m}}. \tag{2.32}$$

The root $\bar{r}=1$ is easily shown (by considering the derivative of $F_{\rm eff}$) to correspond to a stable circular orbit for $\bar{m} < \frac{1}{6}$, while for $\frac{1}{6} < \bar{m} < \frac{1}{3}$ the root $\bar{r} = \frac{3\bar{m}}{1-3\bar{m}} > 1$ corresponds to a (weakly) stable circular orbit. We therefore recover the well-known fact that the innermost stable circular orbit of the Schwarzschild metric is obtained for $\bar{m} = \frac{1}{6}$ which corresponds to a radius $r_0 = \frac{6Gm}{c^2}$.

In Fig. 1 we show $V_{\rm eff}$ obtained by integration of $F_{\rm eff}$ of Eq. (2.22) for $\bar{m} = 0.15 < \frac{1}{6}$ and for $\bar{m} = 0.19 > \frac{1}{6}$.

The plot shows the development of the local maximum of $V_{\rm eff}$ at $\bar{r}=1$ when $\bar{m} > \frac{1}{6}$ and the development of a new minimum at $\bar{r} > 1$. Interestingly, the new minimum is weaker and there is less restoring force for perturbations towards larger $\bar{r}$. Thus, as $\bar{m}$ increases towards the limiting value of $\frac{1}{3}$ (beyond this value there is no circular orbit) the circular orbit becomes less stable and susceptible to destabilization by the repulsive effects of the accelerating expansion.

We now turn to the expansion to investigate how this affects $F_{\rm eff}$ and the potential of the radial geodesics. For definiteness we set $w = -1.2$ ($\bar{t}_* = 6$), which corresponds to a phantom background expansion consistent with current observational constraints [7]. $F_{\rm eff}$ may be obtained in the general-relativistic geodesics when expansion is present by solving the first integral (2.25) for $\dot{\bar{t}}^2$ and substituting it into the radial geodesic (2.24). Assuming a slow shift of the location of the potential minimum with time, we ignore the terms proportional to $\dot{\bar{r}}$ in constructing $F_{\rm eff}$ and $V_{\rm eff}$. This approximation is justified in the next section where we obtain the numerical solution of the full system of the coupled geodesic equations (2.25) and (2.24). The $F_{\rm eff}$ thus obtained is of the form

$$F_{\rm eff} = \bar{r} f^{1/2}\bar{H}'\left[\frac{1+\frac{\bar{m}}{\bar{r}^2(1-3\bar{m})}}{f-\frac{\bar{r}^2\bar{H}^2\bar{m}}{\bar{\omega}_0^2(1-3\bar{m})}}\right] + \left(1-\frac{3\bar{m}}{\bar{r}}\right)\frac{\bar{\omega}_0^2}{\bar{r}^3} - \frac{(1-3\bar{m})\bar{\omega}_0^2}{\bar{r}^2} + \bar{r}\bar{H}^2. \tag{2.33}$$

The corresponding general-relativistic analog of the effective potential $V_{\rm eff}$ may be obtained by numerically integrating $F_{\rm eff}$ as

$$V_{\rm eff}(\bar{r}) = -\int_1^{\bar{r}} F_{\rm eff}(\bar{r}' d\bar{r}'). \tag{2.34}$$

In Fig. 2 we show a plot of $V_{\rm eff}$ for $\bar{m}=0$ and $\bar{m}=0.05$ with the effects of expansion turned off. The plot shows that

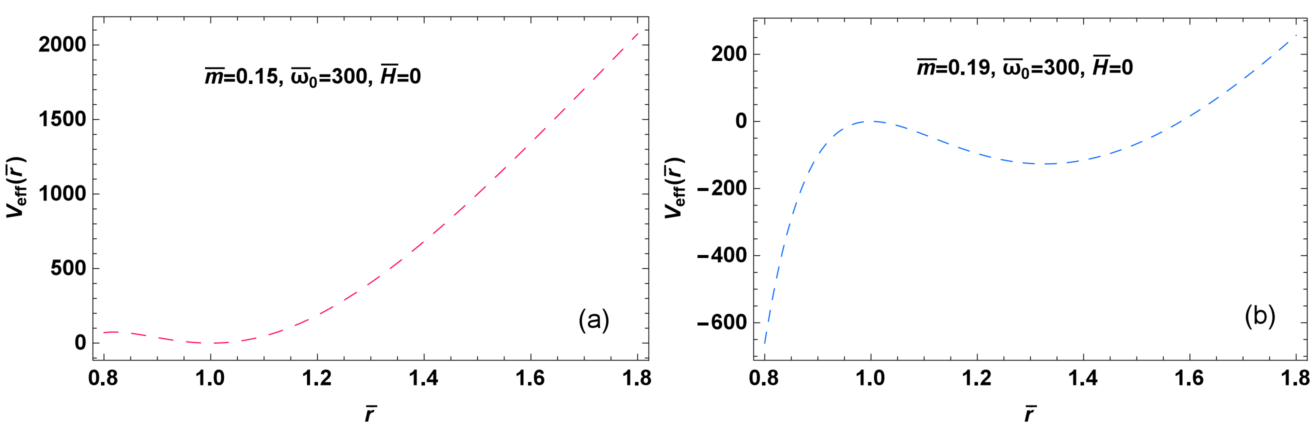

FIG. 1. The general-relativistic analog of the effective potential $V_{\rm eff}$ as a function of $\bar{r}$ in a static universe when $\bar{\omega}_0 = 300$ for $\bar{m} = 0.15 < \frac{1}{6}$ and $\bar{m} = 0.19 > \frac{1}{6}$.

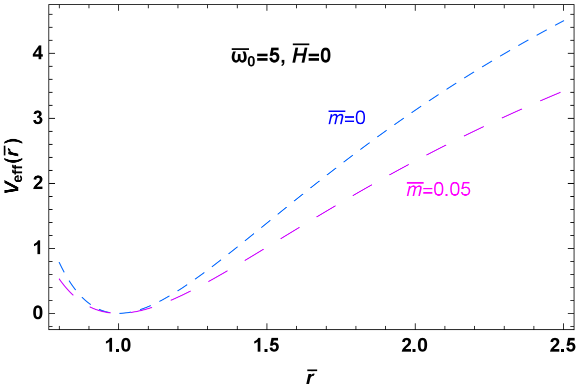

FIG. 2. The general-relativistic analog of the effective potential $V_{\rm eff}$ for $\bar{m} = 0$ and $\bar{m} = 0.05$ with the effects of expansion turned off when $\bar{\omega}_0 = 5$.

the relativistic effects tend to make the bound state weaker and more susceptible to dissociation due to the effects of the expansion. This effect is related to the development of the local maximum (Fig. 1) of the general-relativistic potential for a radius smaller than the radius of the stable orbit (potential minimum), which is also the reason for the existence of an innermost stable circular orbit. Thus, in contrast to naive intuition, the stronger effects of gravity in the relativistic case tend to destabilize rather than stabilize bound systems.

This is also demonstrated in Fig. 3(a) where the effects of the expansion have been turned on ($H \neq 0$, $w = -1.2$) but the time shown is before the bound system dissociation time $\bar{t}_{\rm rip}$. Clearly, the binding power of the relativistic potential has been weakened on large scales in both the relativistic (lower curve) and the Newtonian case (upper curve). Figure 3(b) shows the form of the effective potential for $t = 3.5t_m$.

At that time the system has been dissociated according to the full relativistic analysis, but it remains bound according to the Newtonian approximation.

It is therefore clear that relativistic effects tend to destabilize bound systems, leading to an earlier dissociation (smaller value of $\bar{t}_{\rm rip}$) compared to the predictions in the context of the Newtonian approximation. In the next section we verify this result with a full numerical solution of the geodesic equations (2.24) and (2.25) and we present a quantitative analysis of the magnitude of the relativistic correction required for various bound systems defined by the dimensionless parameters $\bar{\omega}_0$ and $\bar{m}$.

III. QUANTITATIVE ANALYSIS: THE TIME OF BOUND SYSTEM DISSOCIATION

In the previous section we defined the time of dissociation of a bound system as the time when the minimum of $V_{\rm eff}$ disappears due to the effects of the expansion. In the context of a numerical solution of the system of geodesic equations, this definition is not as useful because $F_{\rm eff}$ and $V_{\rm eff}$ are only probed at the location of the solution $\bar{r}(\bar{t})$ with no information about neighboring values of $\bar{r}$ which could determine the binding status and stability of the system.

By comparing the dissociation times predicted by $V_{\rm eff}$ with the form of the trajectories $\bar{r}(\bar{t})$, we concluded that, to within a good approximation, the minimum of $V_{\rm eff}$ disappears when the solution $\bar{r}(\bar{t})$ diverges by about 20% from its initial equilibrium value. We thus use this as a criterion of dissociation when solving the system of geodesic equations numerically. Due to the different nature of this criterion we expect only qualitative agreement between the values of $\bar{t}_{\rm rip}$ obtained from the potential minimum and those obtained from the numerical trajectories $\bar{r}(\bar{t})$. However, as will be discussed below, in most cases the agreement is good even at the quantitative level.

We solved the system of geodesic equations (2.24)–(2.25) with initial conditions corresponding to $\bar{t}_i = 1$ and $\bar{r}_i$ corresponding to the minimum of $V_{\rm eff}$ at $\bar{t} = \bar{t}_i = 1$ (including expansion). This value was (in all cases

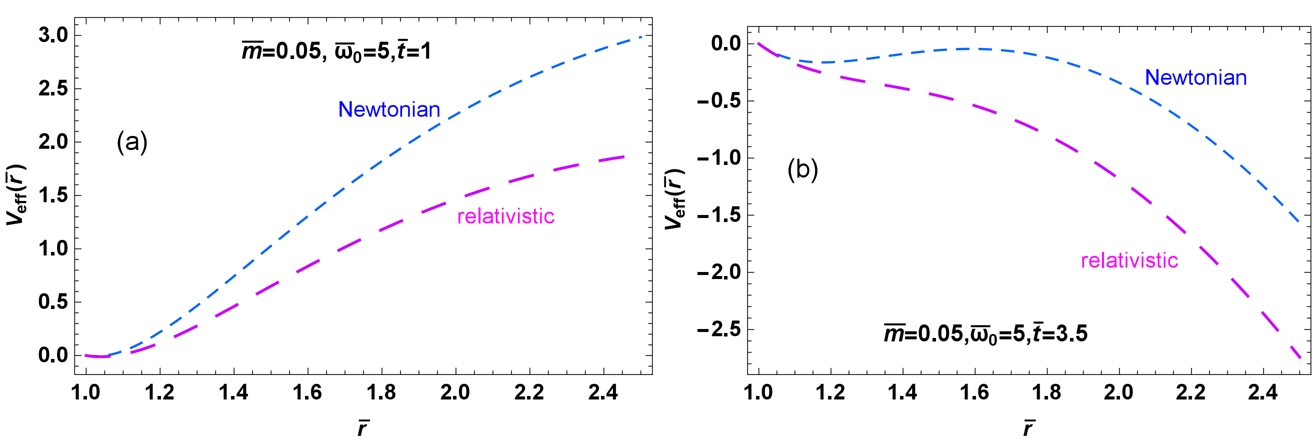

FIG. 3. (a) $V_{\rm eff}$ when the effects of the expansion have been turned on ($H \neq 0$, $w = -1.2$) but the time shown is before the bound system dissociation time $\bar{t}_{\rm rip}$. (b) The form of $V_{\rm eff}$ for $t = 3.5t_m$, where the system has been dissociated according to the full relativistic analysis but it remains bound according to the Newtonian approximation.

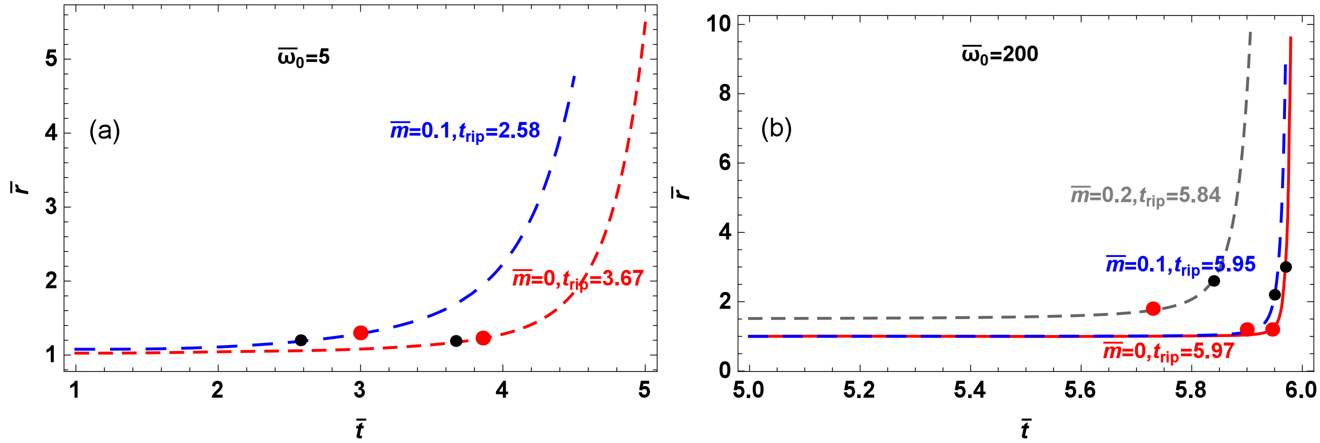

FIG. 4. The radius $\bar{r}$ as a function of $\bar{t}$ when $\bar{\omega}_0 = 5$ and $\bar{\omega}_0 = 200$ for several values of $\bar{m}$. The red points correspond to the time when the size $\bar{r}(t)$ of the system has increased by about 20% compared to its equilibrium value. The black points correspond to the time when the minimum of $V_{\rm eff}$ disappears. Notice that the scale of the $\bar{t}$ axis in the right plot is different and therefore the agreement between red and black points is much better.

considered) close to $\bar{r} = 1$ corresponding to the minimum of $V_{\rm eff}$ without the effects of the expansion. In Fig. 4 we show the solution $\bar{r}(t)$ for $\bar{\omega}_0 = 5$, $\bar{\omega}_0 = 200$ when $\bar{m} = 0.1$, superposed with the corresponding radial function obtained in the Newtonian approximation ($\bar{m} = 0$). The trend for earlier dissociation in the relativistic treatment compared to the Newtonian approach is clear. However, the difference of dissociation times decreases as $\bar{\omega}_0$ increases.

As shown in Fig. 4, the bound system dissociation time $\bar{t}_{\rm rip}$ is well represented by the time when the size $\bar{r}(t)$ of the system has increased by about 20% compared to its equilibrium value. Given the rapid increase of the physical size of the system after dissociation, the assumed relative size increase for dissociation does significantly affect the obtained value for $\bar{t}_{\rm rip}$. This is less accurate for larger systems [smaller $\bar{\omega}_0$ shown in Fig. 4(a)] when the dissociation proceeds more smoothly. Notice also that in all cases $\dot{\bar{r}}$ is small before the dissociation, which justifies the fact that we ignored it in the construction of the general relativistic analog of the effective potential.

Figure 5(a) shows the value of $\bar{t}_{\rm rip}$ as a function of $\bar{\omega}_0$ for various values of $\bar{m}$. The curve for $\bar{m} = 0$ corresponds to the Newtonian limit. As $\bar{m}$ increases, the relativistic correction to the value of $\bar{t}_{\rm rip}$ increases dramatically for low values of $\bar{\omega}_0$ (large massive systems). Therefore, the dissociation of some large and strongly bound systems due to the expansion proceeds significantly earlier than anticipated in the context of the Newtonian approach. This is also demonstrated in Fig. 5(b) where we show $\bar{t}_{\rm rip}$ as a function of $\bar{m}$ for various values of $\bar{\omega}_0$. The thick dots correspond to dissociation times obtained using the numerical solution of the geodesic equations $\bar{r}(t)$, while the lines were obtained using $V_{\rm eff}$ of Eq. (2.34) by finding the time when the potential minimum disappears.

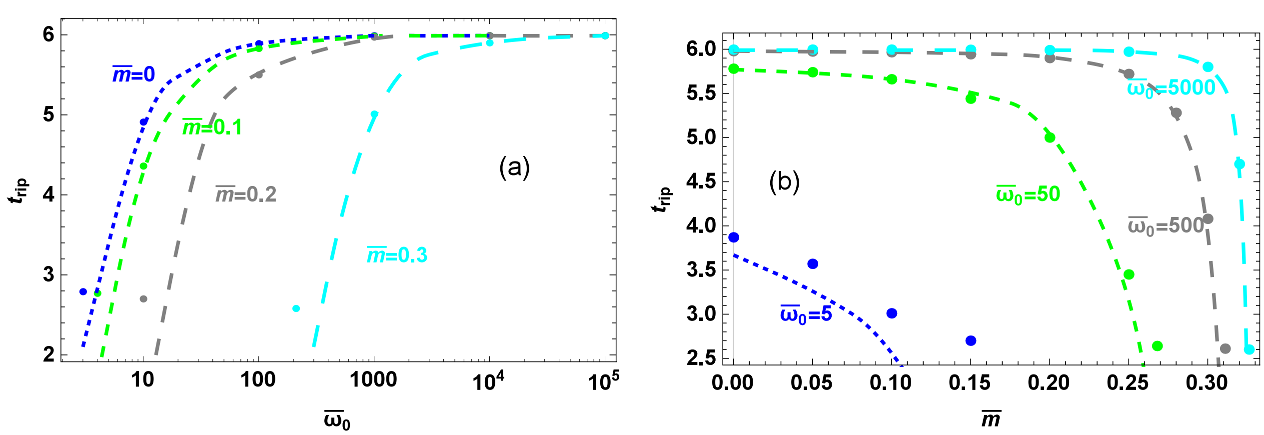

FIG. 5. (a) The value of $\bar{t}_{\rm rip}$ as a function of $\bar{\omega}_0$ for various values of $\bar{m}$. (b) The value of $\bar{t}_{\rm rip}$ as a function of $\bar{m}$ for various values of $\bar{\omega}_0$. The thick dots correspond to dissociation times obtained using the numerical solution of the geodesic equations $r(t)$, while the lines were obtained using the effective potential of Eq. (2.34) by finding the time when the potential minimum disappears.

TABLE I. The parameter values and the corresponding level of relativistic corrections to the dissociation time for some typical bound systems. The last column shows the difference in $\bar{t}_{\rm rip}$ between the Newtonian approximation and the relativistic value $\bar{t}_{{\rm nr}_{\rm rip}} - \bar{t}_{{\rm gr}_{\rm rip}}$, where $\bar{t}_{{\rm nr}_{\rm rip}}$ is the value of $\bar{t}_{\rm rip}$ in the Newtonian approximation and $\bar{t}_{{\rm gr}_{\rm rip}}$ is the relativistic value.

System	Mass ($M_\odot$)	Size (Mpc)	$\bar{\omega}_0$	$\bar{m}$	$\Delta t_{\rm rip}$
Solar System	1.0	2.3×10^{-9}	3.5×10^{6}	2.1×10^{-11}	$<10^{-8}$
Milky Way Galaxy	1.0×10^{12}	1.7×10^{-2}	1.8×10^{2}	2.9×10^{-6}	2.4×10^{-7}
Typical Cluster	1.0×10^{15}	1.0	12	4.9×10^{-5}	5.9×10^{-5}
Accretion Disk (neutron star)	1.5	3.3×10^{-19}	4.3×10^{21}	0.22	$<10^{-8}$
Hypothetical Large Massive	3.0×10^{20}	1.0×10^{2}	9.1	0.15	0.93

Notice however that systems with $\bar{\omega}_0$ larger than about 10^4 (relatively small systems) have dissociation times $\bar{t}_{\rm rip}$ that are practically indistinguishable from the Newtonian approximation, independent of the value of $\bar{m}$. An appreciable deviation of the value of $\bar{t}_{\rm rip}$ from the Newtonian approximation occurs for low values of $\bar{\omega}_0$ (5–100) and large values of $\bar{m}$ $[O(10^{-1})]$. This range of parameters corresponds to large and massive systems (e.g., a size of about 10–100 Mpc and mass 10^6 times larger than a typical cluster of galaxies). Such systems where relativistic corrections are important need to fulfil two conditions.

(1) They need to be large so that the cosmological acceleration repulsive force is important even at early times. Thus $\bar{t}_{\rm rip}$ is relatively small (early dissociation) even at the Newtonian level, allowing for significant change in the context of the relativistic correction.

(2) They also need to be massive so that their Schwarzschild radius (and the innermost stable orbit) is comparable (a few times smaller) to their initial stable orbit radius.

We stress that most cosmological bound systems have a $\bar{m}$ that is much smaller than $\frac{1}{3}$. In particular, for a cluster of galaxies $\bar{m}\simeq10^{-5}$, for a galaxy $\bar{m}\simeq10^{-6}$, and for the Solar System $\bar{m}\simeq10^{-11}$. For such systems the Newtonian approach provides an accurate approach for the dissociation time $\bar{t}_{\rm rip}$.

Even some systems that are considered strongly bound ($\bar{m}\simeq0.1$) such as an accretion disk around a neutron star are not large enough to have an appreciable difference of $\bar{t}_{\rm rip}$ due to relativistic effects (they have a very large $\bar{\omega}_0$). A system with appreciable relativistic corrections of the dissociation time would be a hypothetical bound system with mass 10^{20} $M_\odot$ and size about 100 Mpc (about 10^6 times more massive than a cluster of galaxies).

In Table I we show the parameter values and the corresponding level of relativistic corrections to the dissociation time for some typical bound systems.

Figure 6(a) shows the mass of physical systems as a function of the dimensionless parameter $\bar{\omega}_0$ for various values of $\bar{m}$. Some physical bound systems are also indicated in the plot. Similarly, Fig. 6(b) shows the size of physical systems as a function of the dimensionless parameter $\bar{\omega}_0$ for various values of $\bar{m}$. An accretion disk around a neutron star ($r\simeq50$ km, $M\simeq1.4$ $M_\odot$) is out of the range of these plots as it has $\bar{m}\simeq0.1$ but $\bar{\omega}_0\simeq10^{20}$ [see also Eqs. (2.27) and (2.28)]. As shown in Table I, despite the relatively large value of $\bar{m}$ of such a strongly bound system, its dissociation time would practically be identical to the one derived in the context of the Newtonian approximation due to its relatively small size and large value of $\bar{\omega}_0$.

Relativistic corrections tend to change slowly when the size of a given bound decreases. Such a decrease implies an increase of both $\bar{m}$ and $\bar{\omega}_0$. The parameter values and the corresponding relativistic corrections as the scale of a typical cluster shrinks by a factor of 5 are shown in Table II. Notice that the increase of $\bar{\omega}_0$ appears to be more important during the shrinking a system than the increase of $\bar{m}$, and therefore the relativistic corrections to $\bar{t}_{\rm rip}$ decrease slowly as the size of the bound system is reduced.

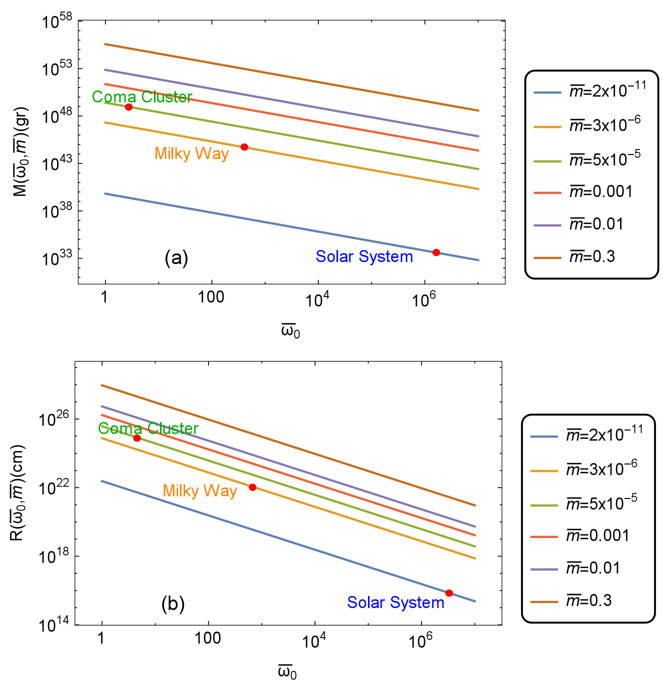

FIG. 6. The mass of physical systems as a function of the dimensionless parameter $\bar{\omega}_0$ for various values of $\bar{m}$ (upper frame) and the size of physical systems as a function of the dimensionless parameter $\bar{\omega}_0$ for various values of $\bar{m}$ (lower frame).

TABLE II. The parameter values and the corresponding level of relativistic corrections to the dissociation time of a typical cluster, when we introduce a rescaling of the size of the system. In the last column we show the difference of the Newtonian $\bar{t}_{\mathrm{nr-rip}}$ minus the corresponding relativistic value. Notice that the relativistic rip occurs slightly earlier as expected, but the difference from the Newtonian value decreases slowly with the rescaling to smaller sizes as the cosmological effects become less important.

System	Mass ($M_\odot$)	Size (Mpc)	$\bar{\omega}_0$	$\bar{m}(\times 10^{-5})$	$\Delta t_{\mathrm{rip}} \times (10^{-5})$
Typical Cluster	10^{15}	1.0	12.4	4.9	5.9
	10^{15}	0.8	17.4	6.1	5.6
	10^{15}	0.6	26.8	8.1	4.6
	10^{15}	0.4	49.2	12	3.8
	10^{15}	0.2	139	24	2.7

IV. CONCLUSION AND DISCUSSION

We have demonstrated that when relativistic effects are taken into account, the dissociation of bound systems in phantom cosmologies occurs earlier than predicted in the Newtonian approximation used by previous studies. The correction in all known bound systems is small. However, there are hypothetical cosmologically large and massive bound systems where the correction is significant.

Our results indicate that the Newtonian approximation is fairly accurate for known bound systems and therefore a relativistic analysis is not required in order to obtain accurate results for the dissociation times for these systems. However, our analysis remains physically interesting and important based on the following arguments:

(i) The correct analysis is the general-relativistic analysis we implemented and it is important to know that this analysis gives credibility to the Newtonian approximation of previous analyses [12]. In analogy, the Friedmann equation has a Newtonian derivation but it cannot be credible until it is verified by a fully general-relativistic analysis. Thus, our analysis is useful and physically relevant even for known bound systems.

(ii) We have shown that there are physical systems that have relativistically derived dissociation times that are very different compared to the Newtonian prediction. Even though such systems are not expected to exist in our Universe, they could in principle exist and therefore their properties are physically interesting.

Interesting extensions of the present analysis include the following:

(1) The analysis of more general classes of geodesics like infalling radial geodesics with no angular momentum which at the time of the big rip are close or even beyond the black hole horizon.

(2) The use of McVittie geodesics to derive the relativistic corrections on the turnaround radius, which is the nonexpanding shell furthest away from the center of a bound structure. In the context of the Newtonian approximation the maximum possible value of the turnaround radius for $w = -1$ (ΛCDM) is equal to $(3GM/\Lambda c^2)$ [31]. The numerical analysis MATHEMATICA files used for the production of the figures may be downloaded from Supplemental Material [32].

[1] L. Perivolaropoulos, Accelerating universe: Observational status and theoretical implications, AIP Conf. Proc. **848**, 698 (2006).
[2] S. M. Carroll, The cosmological constant, Living Rev. Relativ. **4**, 1 (2001).
[3] T. Padmanabhan, Cosmological constant: The weight of the vacuum, Phys. Rep. **380**, 235 (2003).
[4] P. J. E. Peebles and B. Ratra, The cosmological constant and dark energy, Rev. Mod. Phys. **75**, 559 (2003).
[5] E. J. Copeland, M. Sami, and S. Tsujikawa, Dynamics of dark energy, Int. J. Mod. Phys. D **15**, 1753 (2006).
[6] J. Frieman, M. Turner, and D. Huterer, Dark energy and the accelerating universe, Annu. Rev. Astron. Astrophys. **46**, 385 (2008).
[7] N. Said, C. Baccigalupi, M. Martinelli, A. Melchiorri, and A. Silvestri, New constraints on the dark energy equation of state, Phys. Rev. D **88**, 043515 (2013).
[8] P. A. R. Ade *et al.* (Planck Collaboration), Planck 2015 results. XIV. Dark energy and modified gravity, arXiv:1502.01590.
[9] W. Zheng, S. Y. Li, H. Li, J. Q. Xia, M. Li, and T. Lu, Constraints on dark energy from new observations including Pan-STARRS, J. Cosmol. Astropart. Phys. 08 (2014) 030 (2014); , 09 (2014) E01.
[10] E. Piedipalumbo, E. Della Moglie, M. De Laurentis, and P. Scudellaro, High redshift investigation on the dark energy equation of state, Mon. Not. R. Astron. Soc. **441**, 3643 (2014).
[11] V. B. Johri, Phantom cosmologies, Phys. Rev. D **70**, 041303 (2004).
[12] S. Nesseris and L. Perivolaropoulos, The Fate of bound systems in phantom and quintessence cosmologies, Phys. Rev. D **70**, 123529 (2004).
[13] R. R. Caldwell, M. Kamionkowski, and N. N. Weinberg, Phantom energy and cosmic doomsday, Phys. Rev. Lett. **91**, 071301 (2003).

[14] S. Nojiri, S. D. Odintsov, and S. Tsujikawa, Properties of singularities in (phantom) dark energy universe, Phys. Rev. D **71**, 063004 (2005).

[15] L. P. Chimento and R. Lazkoz, On big rip singularities, Mod. Phys. Lett. A **19**, 2479 (2004).

[16] C. Cattoen and M. Visser, Necessary and sufficient conditions for big bangs, bounces, crunches, rips, sudden singularities, and extremality events, Classical Quantum Gravity **22**, 4913 (2005).

[17] R. Nandra, A. Lasenby, and M. Hobson, Dynamics of a spherical object of uniform density in an expanding universe, Phys. Rev. D **88**, 044041 (2013).

[18] C. Gao, X. Chen, Y. G. Shen, and V. Faraoni, Black holes in the universe: Generalized Lemaître-Tolman-Bondi solutions, Phys. Rev. D **84**, 104047 (2011).

[19] R. Nandra, A. N. Lasenby, and M. P. Hobson, The effect of an expanding universe on massive objects, Mon. Not. R. Astron. Soc. **422**, 2945 (2012).

[20] G. C. McVittie, The mass-particle in an expanding universe, Mon. Not. R. Astron. Soc. **93**, 325 (1933); *General Relativity and Cosmology*, 2nd ed. (University of Illinois Press, Champaign, 1962); B. C. Nolan, A point mass in an isotropic universe: Existence, uniqueness and basic properties, Phys. Rev. D **58**, 064006 (1998); Particle and photon orbits in McVittie spacetimes, Classical Quantum Gravity **31**, 235008 (2014); V. Faraoni, Cosmological and black hole apparent horizons, Lect. Notes Phys. **907**, 1 (2015); A. M. da Silva, M. Fontanini, and D. C. Guariento, How the expansion of the Universe determines the causal structure of McVittie spacetimes, Phys. Rev. D **87**, 064030 (2013); K. Lake and M. Abdelqader, More on McVittie's legacy: A Schwarzschild—de Sitter black and white hole embedded in an asymptotically ΛCDM cosmology, Phys. Rev. D **84**, 044045 (2011); N. Kaloper, M. Kleban, and D. Martin, McVittie's legacy: Black holes in an expanding universe, Phys. Rev. D **81**, 104044 (2010); M. Carrera and D. Giulini, On the influence of the global cosmological expansion on the local dynamics in the solar system, arXiv:gr-qc/0602098; V. Faraoni, A. F. Zambrano Moreno, and R. Nandra, Making sense of the bizarre behaviour of horizons in the McVittie spacetime, Phys. Rev. D **85**, 083526 (2012).

[21] R. Moradi, J. T. Firouzjaee, and R. Mansouri, Cosmological black holes: the spherical perfect fluid collapse with pressure in a FRW background, Classical Quantum Gravity **32**, 215001 (2015).

[22] A. Einstein and E. G. Straus, The influence of the expansion of space on the gravitation fields surrounding the individual stars, Rev. Mod. Phys. **17**, 120 (1945).

[23] C. Bona and J. Stela, Swiss cheese, models with pressure Phys. Rev. D **36**, 2915 (1987).

[24] G. A. Baker, Jr., Effects on the structure of the universe of an accelerating expansion, arXiv:astro-ph/0112320.

[25] J. E. Pringle, Accretion discs in astrophysics, Annu. Rev. Astron. Astrophys. **19**, 137 (1981).

[26] M. A. Abramowicz and P. C. Fragile, Foundations of black hole accretion disk theory, Living Rev. Relativ. **16**, 1 (2013).

[27] B. C. Nolan, Particle and photon orbits in McVittie spacetimes, Classical Quantum Gravity **31**, 235008 (2014).

[28] V. Faraoni and A. Jacques, Cosmological expansion and local physics, Phys. Rev. D **76**, 063510 (2007).

[29] P. D. Noerdlinger and V. Petrosian, The effect of cosmological expansion on self-gravitating ensembles of particles, Astrophys. J. **168**, 1 (1971).

[30] R. H. Price, In an expanding universe, what doesn't expand?, arXiv:gr-qc/0508052.

[31] V. Pavlidou and T. N. Tomaras, Where the world stands still: turnaround as a strong test of $\bar{\omega}_0$CDM cosmology, J. Cosmol. Astropart. Phys. 09 (2014) 020.

[32] See Supplemental Material at http://link.aps.org/supplemental/10.1103/PhysRevD.93.123520 for MATHEMATICA files that illustrate the implemented numerical analysis of the present study and the creation of some figures.